

## Electron-positron density-functional theory

E. Boroński\* and R. M. Nieminen

*Department of Physics, University of Jyväskylä, 40100 Jyväskylä, Finland*

(Received 28 October 1985)

A two-component density-functional theory is presented for electron-positron systems. The phase diagram of a two-component Fermi-Coulomb system is discussed, and explicit expressions are derived for exchange-correlation functionals for use in the local-density approximation. The scheme is then applied in a fully self-consistent calculation of electron and positron densities in atomic vacancies in metals, treated in the jellium model. Comparison with conventional calculations, which do not meet true electron-positron self-consistency, reveals considerable changes in the density distributions. However, we demonstrate that there are cancellation effects which render the corresponding changes in observable annihilation characteristics relatively small.

### I. INTRODUCTION

The fundamental question concerning the analysis of positron annihilation in condensed matter is how the electron-positron attraction distorts the electronic structure of the medium which one wants to probe. The attraction leads to a pileup of electron density at the positron, which manifests itself in the annihilation characteristics. For the basic model system, a single delocalized positron in electron gas, this effect is even quantitatively well understood.<sup>1</sup> The total annihilation rate (contact density) increases by a large factor dependent on the electron-density parameter  $r_s$ . However, apart from the short-range screening, the electron states and naturally the mean density remain unperturbed. The  $2\gamma$  angular distribution (momentum density) shows relatively weak changes from the independent-particle limit. For real materials with more or less tightly bound electrons and nonuniform density, the situation is somewhat more complex as the enhancement effects depend on the degree of localization of the electrons. Nevertheless, at least for metallic media, the total annihilation rate (lifetime) of delocalized positrons is reasonably well understood by spatially averaging over the positron probability distribution; the momentum-dependent enhancement effects are more subtle but remain relatively small.<sup>2</sup>

Conceptual difficulties may, however, arise when the positron is localized (trapped), typically at an open-volume lattice defect. It is obvious that the localized positron will now also increase the *average* electron density in the region into which it is confined, and a true calculation requires that the electron and positron distributions are mutually consistent. The problem of short-range screening in this highly nonuniform situation also becomes quite complex.

The conventional way<sup>3-6</sup> through these difficulties, which has met with considerable success in analyzing and predicting annihilation characteristics in various defect situations, is as follows: Treat the short-range screening essentially *locally*, i.e., with a dependence only on the electron density at the instantaneous position of the positron. In metallic media this means that the positron enters the

system as a *neutral* quasiparticle (a positron and its screening cloud). One can then argue that the *average* electron density is not affected by the positron. The positron potential in this approximation is the sum of the Coulomb (Hartree) potential of the electron system and a local electron-positron correlation potential. Consistently, the annihilation rate can be calculated through the local-density profile and the enhancement-factor data from homogeneous systems.

This picture clearly breaks down in two cases. Firstly, in some instances the positron may be detached from its screening cloud, and therefore the local-density approximation (LDA) becomes invalid. The image-potential-induced surface state<sup>7</sup> is a case in point. Secondly, the degree of positron localization can be such that the spatial extent of the screening cloud is comparable to the extent of the trapped positron state. Then it is clear that the electron density near the positron will be seriously distorted, and a self-consistent calculation is required.

Two-component density-functional theory<sup>8-10</sup> (DFT) provides a systematic way of treating the latter situation. We may regard the system of a localized positron and electrons as one made of two interpenetrating nonuniform liquids, characterized by their density distributions  $n_+(\mathbf{r})$  and  $n_-(\mathbf{r})$ . The formalism of one-component DFT can be generalized to this case, and the self-consistency *between*  $n_+(\mathbf{r})$  and  $n_-(\mathbf{r})$  can be built in from the beginning. Exchange and correlation effects are described in terms of appropriate density functionals, which are approximated by using data from uniform two-component plasmas. On the basis of DFT, this is completely legitimate (although admittedly somewhat artificial; see discussion of self-interaction and nonlocal effects below) also in the case of a *single* localized positron. With the advent of high-intensity positron beams,<sup>11</sup> the laboratory realization of *many*-positron systems is actually now becoming a possibility, and the methods will find several interesting applications there. Naturally, the techniques also lend themselves for application into nonuniform *electron-hole* plasmas<sup>12,13</sup> with many intriguing properties. However, electron-hole systems are often dominated by band-structure (i.e., effective-mass and anisotropy) effects,

whereas electron-positron plasmas are much simpler in this sense.

The purpose of this paper is to provide the framework and applicable input data for practical calculations within the two-component DFT. In particular, we shall discuss the electron-positron correlation functional and the enhancement (screening) effects in two-component systems, with practical formulas for numerical applications. Moreover, we shall report on calculations for an important model system, a positron trapped at a simple metal vacancy, and compare the results with those of the conventional approach.

The rest of the paper is organized as follows: In Sec. II we outline the two-component DFT. Section III contains a detailed discussion of the phase diagram of a two-component Coulomb-Fermi system. The correlation functionals and density-enhancement factors are constructed in Sec. IV, and Sec. V reports the results of the model calculations for vacancies. A short summary is given in Sec. VI.

## II. DENSITY-FUNCTIONAL THEORY

The total energy of system of interacting electrons and positrons moving in an external potential  $V_{\text{ext}}$  can be written in terms of the following functional,<sup>7</sup>

$$E[n_+, n_-] = F[n_+] + F[n_-] + \int d\mathbf{r} V_{\text{ext}}(\mathbf{r})[n_-(\mathbf{r}) - n_+(\mathbf{r})] - \int d\mathbf{r} \int d\mathbf{r}' \frac{n_-(\mathbf{r})n_+(\mathbf{r}')}{|\mathbf{r} - \mathbf{r}'|} + E_c^{e-p}[n_+, n_-], \quad (1)$$

where  $F[n]$  denotes the one-component functional<sup>8</sup> for electrons (or positrons) only and  $E_c^{e-p}[n_+, n_-]$  is the electron-positron correlation-energy functional. The variational Kohn-Sham procedure applied to  $E[n_+, n_-]$  leads to a set of one-particle equations for electrons and positrons (atomic units are used throughout; the particles masses are equal to the bare electron mass:  $m_+ = m_- = m$ ),

$$-\frac{1}{2}\nabla^2\psi_i(\mathbf{r}) + \left\{ \mu_{\text{xc}}(n_-(\mathbf{r})) + \phi(\mathbf{r}) + \frac{\delta E_c^{e-p}[n_+, n_-]}{\delta n_-(\mathbf{r})} \right\} \psi_i(\mathbf{r}) = \varepsilon_i \psi_i(\mathbf{r}), \quad (2)$$

$$-\frac{1}{2}\nabla^2\psi_i^+(\mathbf{r}) + \left\{ \mu_{\text{xc}}(n_+(\mathbf{r})) - \phi(\mathbf{r}) + \frac{\delta E_c^{e-p}[n_+, n_-]}{\delta n_+(\mathbf{r})} \right\} \psi_i^+(\mathbf{r}) = \varepsilon_i^+ \psi_i^+(\mathbf{r}), \quad (3)$$

where  $\mu_{\text{xc}}$  is the exchange-correlation potential for each component,

$$\phi(\mathbf{r}) = \int d\mathbf{r}' \frac{n_-(\mathbf{r}') - n_+(\mathbf{r}') - n_0(\mathbf{r}')}{|\mathbf{r} - \mathbf{r}'|} \quad (4)$$

is the Hartree-Coulomb potential, and

$$n_-(\mathbf{r}) = \sum_{\varepsilon_i < \varepsilon_F} |\psi_i(\mathbf{r})|^2, \quad n_+ = \sum_i^{N_+} |\psi_i^+(\mathbf{r})|^2, \quad (5)$$

and  $n_0(\mathbf{r})$  denotes the density of positive charge providing the external potential. Equations (2)–(5) should be solved self-consistently;  $\varepsilon_F$  in Eq. (5) is the electron Fermi energy and  $N_+$  the number of positrons.

## III. THE GROUND-STATE ENERGY OF A HOMOGENEOUS ELECTRON-POSITRON SYSTEM

In order to construct correlation potentials for the inhomogeneous electron-positron system, we first discuss the energies of homogeneous systems. As the results are to be used in our density-functional formulation, we consider the total energy  $E_T$  of the system of  $N_-$  electrons and  $N_+$  positrons as consisting of the following parts:

$$E_T = E_k + E_x + E_c. \quad (6)$$

$E_k$  and  $E_x$  are the noninteracting kinetic and exchange energies, respectively, and  $E_c$  is the correlation energy. It contains the electron-electron, positron-positron, and electron-positron correlations:

$$E_c = E_c^{e-e} + E_c^{p-p} + E_c^{e-p}. \quad (7)$$

The correlation energy *per unit volume* can be expressed as

$$E_c^V = n_- \varepsilon_c^{e-e}(n_-) + n_+ \varepsilon_c^{p-p}(n_+) + E_{\text{V}}^{e-p}(n_+, n_-), \quad (8)$$

where  $\varepsilon_c^{e-e}$  and  $\varepsilon_c^{p-p}$  are the respective correlations *per particle*. Recently, accurate values for  $\varepsilon_c^{e-e}$  were calculated using Monte Carlo methods by Ceperley and Alder,<sup>14</sup> and these results will be used below. We would like to emphasize here that  $E_{\text{V}}^{e-p}(n_+, n_-)$  cannot be generally expressed by terms of the *energy per particle* in the same sense as  $\varepsilon_c^{e-e}$  or  $\varepsilon_c^{p-p}$ . It is possible only for  $n_+ \rightarrow 0$  [ $E_{\text{V}}^{e-p} \rightarrow n_+ \varepsilon_c^{e-p}(n_-)$ ] or  $n_+ = n_-$  [ $E_{\text{V}}^{e-p} = n \varepsilon_c^{e-p}(n)$ , where  $n$  is the density of electron-positron pairs]. The few results which can suit our purposes refer just to these limits. There are also some recent results<sup>15</sup> for  $n_+ = \frac{1}{2}n_-$ .

The first case ( $n_+ \rightarrow 0$ ) corresponds to one positron in an electron gas. The paper of Arponen and Pajanne<sup>1</sup> provides electron-positron correlation energies for the whole metallic-density regime and also for the limit  $r_s \rightarrow \infty$ , where the correlation energy reaches the value of the energy of the  $\text{Ps}^-$  ion. Their curve is reproduced in Fig. 2, and the suitable formulas interpolating it for all values of  $r_s$  are presented in Appendix A.

The next case more familiar from semiconductor physics is one where the numbers of electrons and positrons are equal ( $n_+ = n_-$ ), i.e., a particular case of electron-hole plasmas with  $m_+ = m_-$ . Since the properties of this system have not been calculated as consistently as for one positron in electron gas and are not known for the whole range of  $r_s$ , we discuss them more carefully, separating out density regions with very different physical behavior.

### A. Metallic-density regime

For the compensated case  $n_+ = n_-$ , the metallic region is relatively well described. We discuss two approaches dealing with the two-component plasma where correlation energies are calculated, the first given by Vashishta, Bhattacharyya, and Singwi (VBS),<sup>12</sup> and the second presented recently by Lantto *et al.*<sup>15</sup>

The VBS approach is based on the theory of electron correlations by Singwi *et al.*,<sup>16</sup> generalized to a two-component system of electrons and holes in a semiconductor. There are also earlier generalizations of the theory to a positron in homogeneous electron gas.<sup>17</sup> These formulations take into account the multiple interaction of the two components in a self-consistent way. The results seem to be satisfactory for small  $r_s$  and for a considerable part of the metallic-density range. However, for  $r_s \gtrsim 4.5$  they begin to exhibit divergencies. Although Bhattacharyya and Singwi<sup>18</sup> tried to remove these by subtracting a part of positron-electron correlations in a parameter-dependent approach, their method, however, has deficiencies and was not used in the VBS calculations.

Lantto's<sup>15</sup> results are based on the hypernetted-chain (HNC) approximation of many-body theory. These methods have given interesting results for the electron liquid.<sup>19,20</sup> Also, the results for one given positron in a homogeneous electron gas do not exhibit any divergencies over the range of  $r_s$ .<sup>21</sup> Therefore, in spite of the fact that this method provides slightly higher values of total energy than VBS (Fig. 2), we used these results below. In Fig. 1

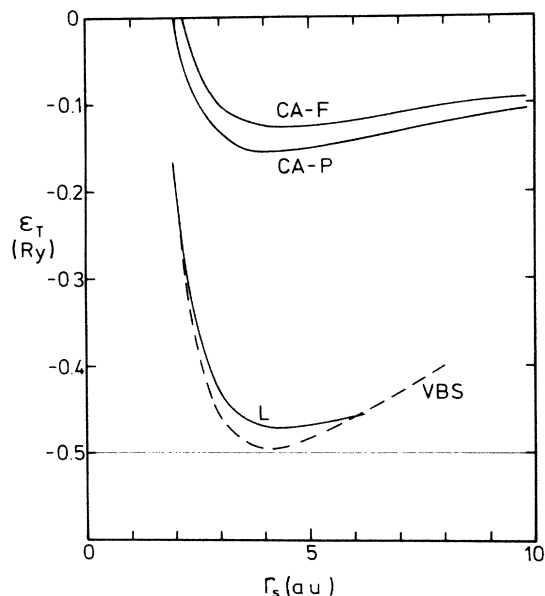


FIG. 1. Total energy of positron-electron ( $n_+ = n_-$ ) and pure electron system vs  $r_s$  for metallic densities. L and VBS denote the results of Lantto (Ref. 15) and Vashishta, Bhattacharyya, and Singwi (Ref. 12) per  $e$ - $p$  pair, respectively. CA-F and CA-P denote the results for the total energy per electron of the pure electron gas in the ferromagnetic and paramagnetic state, obtained by Ceperley and Alder (Ref. 14).

we also present the total energy per electron-positron pair versus  $r_s$  using the VBS and Lantto results for the correlation energies. Both curves exhibit minima around  $r_s \approx 4$ . The VBS-curve minimum almost reaches the value of  $-0.5$  Ry, which is the energy of Ps atom (or exciton).

For small  $r_s$  the curves come close to each other and the electron-positron correlation energies tend to the corresponding values (Fig. 2) for electron-correlation energies calculated by Ceperley *et al.*<sup>14</sup> It seems that for the  $n_+ = n_-$  plasma the correlation energies already around  $r_s \sim 1$  become independent of the particle charges.

As  $r_s$  increases the numerical convergence of both methods becomes slow and for  $r_s > 8$  in VBS and for  $r_s > 6$  in Lantto's calculations the results become divergent or unstable, respectively. It is not surprising for the VBS theory; for the case of one positron similar theories have failed.<sup>17</sup> It is, however, a more unexpected result of Lantto's approach. The HNC methods have generally worked well for greater  $r_s$ , as was shown, e.g., for one positron in an electron gas.<sup>21</sup> The instabilities may advocate the appearance of states which cannot be described by similar wave functions as for smaller  $r_s$ , and we expect that some "bound" states can be created. Such bound states are forbidden for one positron among many, because of the strong scattering in the positron-electron sys-

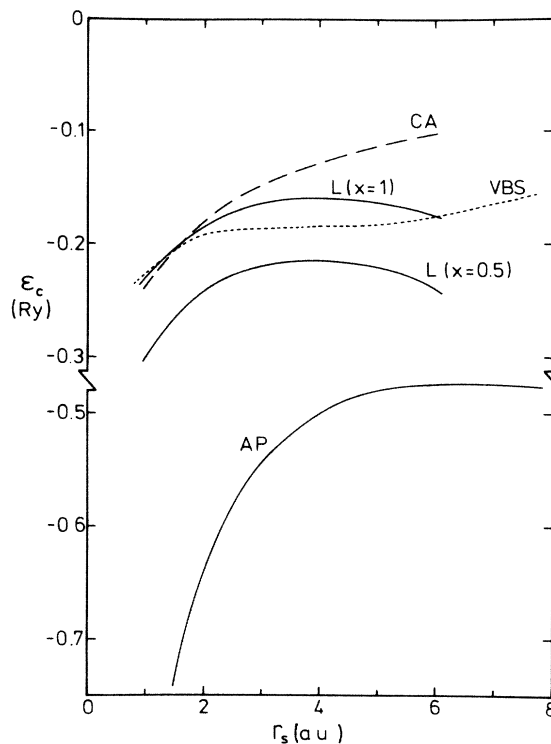


FIG. 2. Positron-electron correlation energy vs  $r_s$  in positron-electron system of different  $n_+/n_-$  ratios. The curve for one positron in a homogeneous electron gas (Ref. 1) is denoted by AP. The results of Lantto for  $n_+/n_- = 1$  and  $0.5$  are denoted by L. The dotted curve presents the results of Vashishta, Bhattacharyya, and Singwi (Ref. 10) for  $n_+/n_- = 1$ . For comparison, the correlation energy in the pure electron gas (per electron-electron pair) is also presented (CA) (Ref. 14).

tem,<sup>22</sup> but for the case  $n_+ = n_-$  pairing of particles for some large  $r_s$  may be possible. Probably true Ps-like bound states cannot appear at once, but rather states of very small energy, with wave functions of Cooper or hydrogenic type. Brinkman and Rice<sup>23</sup> found such solutions for  $r_s$  in the metallic-density regime, using only a model potential which did not take into account strong electron-positron (-hole) correlations. Unfortunately, the VBS and HNC schemes are not adapted to take into account the possibility of creating bound states, and may therefore fail in this region.

It is worthwhile, however, to pay attention (Fig. 2) to the trend of both the correlation energy curves for  $r_s > 4$ . While the VBS curve shows no tendency to bend down toward the Ps (or excitonic) value of energy, Lantto's curve starting from  $r_s \approx 4$  goes down. This is another reason which, in our opinion, makes the latter results more trustworthy.

For  $r_s > 6$ , with diminishing kinetic energy and correlations between particles of like charge, certainly, the "bound states" start to dominate. Some authors<sup>23,24</sup> even expect for  $r_s \approx 10$  a Mott-type phase transition. However, before discussing it we turn to the case of a very dilute positron-electron system.

### B. Molecular phase

As has been indicated by Brinkman *et al.*,<sup>23,25</sup> there is a possibility of binding four particles (two Ps atoms or two excitons) into a neutral molecule. The binding energy of this molecule is 0.029 of the positronium rydberg,<sup>25</sup> which gives the total energy of the molecule as  $\sim 1.0145$  Ry ( $-0.50725$  Ry per pair).

The mean interpositron distance is about 6.94 a.u.,<sup>26</sup> and we can regard the molecule as two weakly coupled Ps atoms (excitons). A sufficiently dilute neutral ( $N_+ = N_- = N$ ) positron-electron system can be built from such  $\text{Ps}_2$  molecules. The interactions between molecules are of the van der Waals type, repulsive for small and attractive for greater distances. For large  $r_s$  some authors<sup>27</sup> expect the possibility of building greater complexes of molecules, although Brinkman and Rice<sup>23</sup> consider it impossible. In our opinion, even if such complexes can exist, the change in the binding energy will be so small that for our practical purposes there is no need to consider them.

More important is the exchange energy. Because of the very small binding between particles within the molecule, it can exist only when electrons and positrons are paired into singlet states. Thus there is no exchange between electrons (and positrons) inside the molecule. However, the electron (or positron) in this molecule can "see" all the  $N - 2$  remaining electrons (positrons) which have both spins down and up. We assume that the exchange energy, which depends only on wave-function properties, is the same as in noninteracting electron gas. Thus the exchange energy  $\epsilon_x$  does not contribute to the molecular energy  $\epsilon_{\text{Ps}_2}$  but should be added to the total energy of the system in comparison with the energy of separate molecules. It is the main factor responsible for the interaction between the molecules. Thus the total energy per

electron-positron pair in the molecular phase consists of the following terms,

$$\epsilon_T = \frac{1}{2} \epsilon_{\text{Ps}_2} + \epsilon_x + \epsilon_k + \Delta \epsilon_c^{e-e, p-p} + \Delta \epsilon_c^{e-p}, \quad (9)$$

where  $\epsilon_k$  is the kinetic energy and  $\Delta \epsilon_c^{e-e, p-p}$ , and  $\Delta \epsilon_c^{e-p}$  are correlation contributions to the interaction between the molecules.

Since the distance between molecules is large,  $\Delta \epsilon_c^{e-e, p-p}$  and  $\Delta \epsilon_c^{e-p}$  are small and, in addition, cancel against the kinetic energy. Besides, our calculations based on wave functions given by Akimoto and Hanamura<sup>26</sup> and made within the LDA show that the correlations within the molecule are almost the same as for electron gas of  $r_s \sim 15$ , thus confirming that  $\Delta \epsilon_c^{e-e, p-p}$  should be weak.  $\Delta \epsilon_c^{e-p}$  is also small, as the electron-positron interaction is well screened within a molecule. The above considerations provide us with the following formulas for the molecular region,

$$\epsilon_T \approx \frac{1}{2} \epsilon_{\text{Ps}_2} + \epsilon_x \quad (10)$$

and [cf. Eqs. (6) and (7)]

$$\epsilon_c^{e-p} = \frac{1}{2} \epsilon_{\text{Ps}_2} - \epsilon_c^{e-e} - \epsilon_c^{p-p}. \quad (11)$$

Thus, for  $r_s \rightarrow \infty$ ,  $\epsilon_T$  approaches the value  $\frac{1}{2} \epsilon_{\text{Ps}_2}$  from below as  $-r_s^{-1}$ . The electron-positron correlation energy becomes larger in absolute value with increasing  $r_s$ , slowly (as  $2\epsilon_c^{e-e}$ ) approaching the value  $\frac{1}{2} \epsilon_{\text{Ps}_2}$ .

### C. Intermediate region

As shown by Brinkman and Rice,<sup>23</sup> the description of the molecular state in terms of a weakly interacting gas of molecules breaks down at  $r_s \approx 13.8$  when the energy gained by the formation of molecules is overcome by the repulsive interactions and the molecule can decay into two separate "quasipositronium" atoms. We use the term "quasipositronium" rather than positronium, since Ps cannot exist for this range of  $r_s$  as an isolated atom. According to some authors,<sup>28</sup> such bound states can appear when increasing  $r_s$  at the end of the metallic region (see Sec. III A). Brinkman and Rice,<sup>23</sup> using the Mott criterion for the metal-nonmetal transition, found that for  $r_s \approx 9.8$  a transition in the compensated electron-hole plasmas can take place. Within the range  $9.8 \lesssim r_s \lesssim 14$  we deal with an "excitonic phase," in the language of electron-hole systems. In this phase the positron-electron system can exist as separate pairs in which particles are strongly bound, but with also strong interaction between the pairs. Therefore and according to the arguments of Kohn and Majumdar,<sup>29</sup> we are of the opinion that there should be no sharp transition at a definite density, the more so as this is not the case of binding of a light particle to a heavy one, but both particles are light and recoil effects further smoothen the transition. The same arguments can be used also for the transition from the "excitonic" to the molecular phase.

Based on these considerations, and bearing in mind that the correlation-energy curve in the metallic-density regime goes down with  $r_s$ , it seems reasonable to obtain the

values for correlation energy  $\epsilon_c^{e-p}$  in the intermediate region simply by smooth interpolation between the metallic and molecular phases. We expect that the error of this interpolation does not exceed the errors in the calculated values for the metallic or molecular phases.

The values for the total energy in this region are obtained by summing:

$$\epsilon_T = \epsilon_k = \epsilon_x + 2\epsilon_c^{e-e} + \epsilon_c^{e-p}. \quad (12)$$

The corresponding curves for the total and electron-positron correlation energies per pair are presented for all values of  $r_s$  in Fig. 3, and interpolation formulas for the whole range of  $r_s$  are given in Appendix A. It is interesting that the maximum of both ( $n_+ = n_-$  and  $n_+ \rightarrow 0$ ) curves lies in the center of the metallic-density regime. The total-energy curve has a deep minimum close to  $r_s \cong 14$ , just in the region where one can expect a transition from separated pairs of particles into  $\text{Ps}_2$  molecules. This minimum is considerably deeper than the one around  $r_s = 4$ . Around  $r_s \cong 6$ , a maximum in the total energy separates the regions of stability.

We would like to emphasize that both (total- and correlation-energy) curves for the case  $n_+ = n_-$  are presented here for the first time for the entire range of density, and despite partly qualitative considerations used in order to complete them, may be used for further calculations, e.g., for constructing correlation potentials for two-component systems.

#### IV. CORRELATION-ENERGY FUNCTIONAL AND ENHANCEMENT FACTOR

For the general case of nonequal electron and positron densities, one should recall that the electron-positron correlation-energy functional is presented as discussed in Sec. II, in terms of the energy per *unit volume* rather than *per particle*.

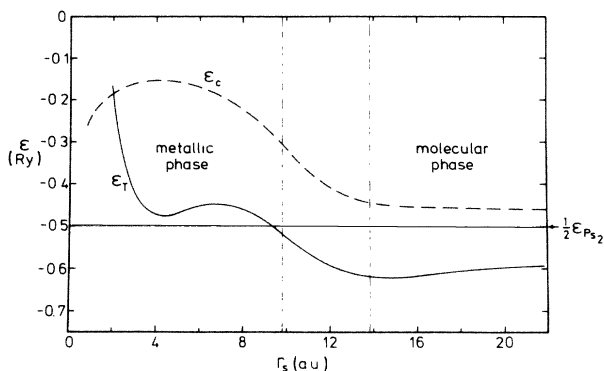


FIG. 3. The full diagram of total and positron-electron correlation energies (per positron-electron pair) vs  $r_s$  for the compensated ( $n_+ = n_-$ ) positron-electron system. The division of the diagram into separate metallic and molecular phases is denoted (see discussion in Sec. III). The energy of the Ps atom is  $-0.5$  Ry and that of the  $\text{Ps}_2$  molecule (per  $e-p$  pair) is  $-0.50725$  Ry.

Only for the limits  $n_+ \rightarrow 0$  and  $n_+ = n_-$  can the total correlation-energy functionals (see Fig. 4) be expressed in the LDA by the familiar formulas,

$$E_c^{e-p}[n_+, n_-] \xrightarrow{n_+ \rightarrow 0} \int d\mathbf{r} n_+(\mathbf{r}) \epsilon_c^{e-p}(n_+ \rightarrow 0, n_-(\mathbf{r})), \quad (13)$$

where  $\epsilon_c^{e-p}(n_+ \rightarrow 0, n_-) = \epsilon_{\text{AP}}(n_-)$  is the known result of the theory of Arponen and Pajanne's,<sup>1</sup> and

$$E_c^{e-p}[n_+, n_-] \Big|_{n_+ = n_-} = \int d\mathbf{r} n(\mathbf{r}) \epsilon_c^{e-p}(n_+(\mathbf{r}), n_-(\mathbf{r})) \Big|_{n_+ = n_-},$$

where

$$\epsilon_c^{e-p}(n_+, n_-) \Big|_{n_+ = n_-} = \epsilon_L(n)$$

is the energy per pair from the Lantto approach<sup>15</sup> complemented in Sec. II of this paper. On the basis of this knowledge we construct the surface of energies per unit volume  $E_V^{e-p}(n_+, n_-)$  throughout the  $(n_+, n_-)$  plane.

The correlation potentials, defined as functional derivatives of the correlation energies

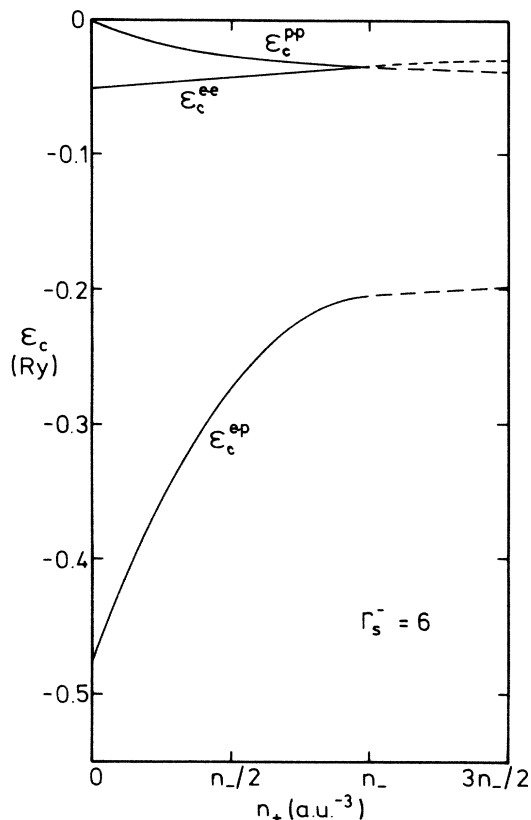


FIG. 4. Components of total correlation energy  $\epsilon_c$  (per electron), in the positron-electron system of varying positron density  $n_+$ . The electron density corresponds to  $r_s = 6$ .  $\epsilon_c^{p-p}$  is the positron-positron correlation energy (per positron),  $\epsilon_c^{e-e}$  is the electron-electron correlation energy (per electron), and  $\epsilon_c^{e-p}$  is the electron-positron correlation energy, defined as  $\epsilon_c^{e-p} = n_-(\epsilon_c - \epsilon_c^{e-e})/n_+ - \epsilon_c^{p-p}$ .

$$\begin{aligned}\mu_+[n_+,n_-] &= \frac{\delta E_c^{e-p}[n_+,n_-]}{\delta n_+}, \\ \mu_-[n_+,n_-] &= \frac{\delta E_c^{e-p}[n_+,n_-]}{\delta n_-}\end{aligned}\quad (14)$$

become partial derivatives of  $E_V^{e-p}(n_+,n_-)$  along the  $n_+,n_-$  directions,

$$\begin{aligned}\mu_-(n_+,n_-) &= \frac{\partial E_V^{e-p}(n_+,n_-)}{\partial n_+}, \\ \mu_-(n_+,n_-) &= \frac{\partial E_V^{e-p}(n_+,n_-)}{\partial n_-}.\end{aligned}\quad (15)$$

Since for  $n_+ \rightarrow 0$ ,  $E_V^{e-p}$  behaves as  $n_+ \epsilon_{AP}(n_-)$ , the slope of the surface (parallel to the  $n_+$  axis) close to the  $n_-$  axis is equal to  $\epsilon_{AP}(n_-)$ . In turn, for  $n_+ = n_- = n$ ,  $E_V$  equals  $n \epsilon_L(n)$ . The surface  $E_V^{e-p}(n_+,n_-)$  is, of course, symmetric with respect to  $n_+$  and  $n_-$ . Taking this fact into account and assuming the continuity of partial derivatives in all directions, one obtains

$$\begin{aligned}\mu_-(n_+,n_-)_{n_+=n_-=n} &= \mu_+(n_+,n_-)_{n_+=n_-=n} \\ &= \frac{1}{2} \frac{\partial}{\partial n} [n \epsilon_L(n)] = \mu_0(n).\end{aligned}\quad (16)$$

Let us now assume the following analytic form for  $E_V^{e-p}(n_+,n_-)$ ,<sup>30</sup>

$$E_V^{e-p}(n_+,n_-) = n_< [a(n_>) + b(n_>)n_< + c(n_>)n_<^2], \quad (17)$$

where  $n_<$  ( $n_>$ ) denotes the smaller (greater) of the densities  $n_+$  and  $n_-$ . Then the unknown coefficients  $a(n)$ ,  $b(n)$ , and  $c(n)$  can be found by solving the following set of equations:

$$\begin{aligned}\left. \frac{\partial E_V^{e-p}(n_+,n_-)}{\partial n_+} \right|_{n_+=n_-=n} &= \mu_0(n), \\ \left. \frac{\partial E_V^{e-p}(n_+,n_-)}{\partial n_+} \right|_{n_+ \rightarrow 0} &= \epsilon_{AP}(n_-), \\ E_V^{e-p}(n_+,n_-) \Big|_{n_+=n_-=n} &= n \epsilon_L(n).\end{aligned}\quad (18)$$

The solution is

$$\begin{aligned}a(n) &= \epsilon_{AP}(n), \\ b(n) &= \frac{1}{n} [3\epsilon_L(n) - 2\epsilon_{AP}(n) - \mu_0(n)], \\ c(n) &= \frac{1}{n^2} [\mu_0(n) + \epsilon_{AP}(n) - 2\epsilon_L(n)].\end{aligned}\quad (19)$$

Thus, applying data from the correlation energies for  $n_+ \rightarrow 0$  and  $N_+ = n_-$  and using the symmetry properties of  $E_V^{e-p}(n_+,n_-)$ , we can provide correlation energies for the whole density plane ( $n_+,n_-$ ). The form (17) is admittedly arbitrary but useful for practical purposes. In Fig. 5 a few cross sections through  $E_V^{e-p}(n_+,n_-)$  are presented.

The correlation potentials needed for solving the self-consistent equations (2) and (3) are simple derivatives of (17) with respect to  $n_+$  and  $n_-$ . They are continuous and

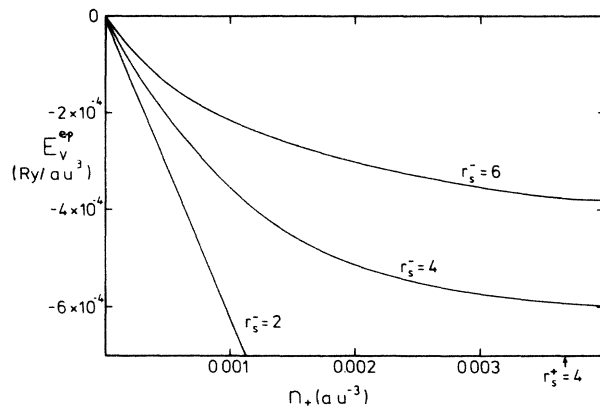


FIG. 5. Values of the positron-electron correlation energy (per unit volume)  $E_V^{e-p}(n_+,n_-)$  vs  $n_+$  for various values of  $n_-$ .

well behaved at  $n_+ = n_-$ . Some examples of values for these potentials are presented in Fig. 6. One can see that for a given value of the electron density  $n_-$ , the magnitude of the correlation potential  $\mu_-$  for electrons reaches a maximum in the region where the positron density is greater than  $n_-$  and, in turn, the potential for positrons  $\mu_+$  becomes larger with  $n_+$  decreasing below  $n_-$ . Thus, the correlation forces between unlike particles in inhomogeneous systems where, e.g., positrons are clustering around a negative potential and electrons are repelled by it, will act towards smoothing the densities.

For lower densities  $n_+$  and  $n_-$ , an unexpected feature emerges: the potentials may become slightly positive.

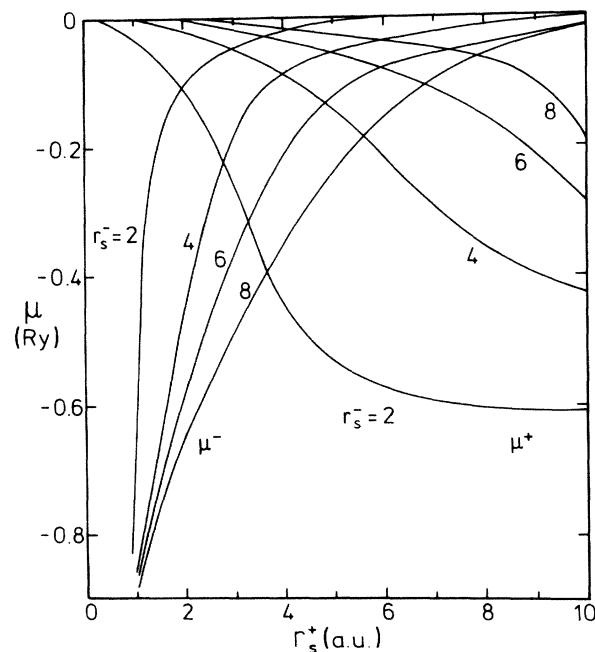


FIG. 6. Positron-electron correlation potentials vs  $r_s^+$  for various electron densities ( $r_s^- = 2, 4, 6, 8$ ). Potentials for electrons are denoted  $\mu^-$  and potentials for positrons are denoted  $\mu^+$ .

This results from the special character of the Arponen-Pajanne<sup>1</sup> correlation-energy curve. The derivative of this curve is positive already for  $r_s \gtrsim 6$ . Thus, for sufficiently small  $n_+$ ,

$$\mu_- \approx \frac{\partial}{\partial n_-} n_+ \varepsilon_{\text{AP}}(n_-) = n_+ \frac{\partial}{\partial n_-} \varepsilon_{\text{AP}}(n_-) > 0. \quad (20)$$

This effect does not appear if other correlation-energy values<sup>17</sup> are used, since they tend to the limit  $-0.5$  Ry from below. As  $\mu \rightarrow 0$  only for very low density and the corresponding potentials are very small, for such applications as, for instance, positron annihilation in point defects of metals, the effect is completely negligible.

The key observable signal is the annihilation rate proportional to the overlap of electron and positron densities. When  $n_+(\mathbf{r})$  and  $n_-(\mathbf{r})$  are known, the conventional way of calculating annihilation rates has been based on the application of the local-density formula

$$\lambda = \pi r_0^2 c \int d\mathbf{r} n_+(\mathbf{r}) n_-(\mathbf{r}) \Gamma(n_-(\mathbf{r})), \quad (21)$$

where

$$\Gamma(n_-) \cong \left[ 1 + \frac{r_s^3(n_-) + 10}{6} \right] \quad (22)$$

is the Brandt-Reinheimer expression<sup>31</sup> approximating the electron-density enhancement at the positron position, valid for a single positron in an electron gas<sup>1</sup> ( $n_+ \rightarrow 0$ ). The constants  $r_0$  and  $c$  appearing in Eq. (21) are the electron radius and speed of light, respectively. Within the two-component formalism one should replace Eq. (21) by

$$\lambda = \pi r_0^2 c \int d\mathbf{r} n_+(\mathbf{r}) n_-(\mathbf{r}) g(0; n_+, n_-) \quad (23)$$

using a new formula for the contact density, i.e., the value of the pair correlation function at the origin  $g(0; n_+, n_-)$  which properly describes enhancement effects in the positron-electron mixture. Recently, values for  $g(0; n_+, n_-)$  have been calculated by Lantto<sup>15</sup> for  $n_+ \rightarrow 0$ ,  $n_+ = \frac{1}{2}n_-$ , and  $n_+ = n_-$  (see Table I). Since for practical applications  $g(0; n_+, n_-)$  must be known for all values of  $n_+$  and  $n_-$ , we use an interpolation scheme similar to the one used for  $E_V^{e-p}(n_+, n_-)$ .

Thus,

$$g(0; n_+, n_-) = a(n_+) n_-^3 + b(n_+) n_-^2 + c(n_+) n_- + g_0(n_+) \quad \text{for } n_+ \lesssim n_-, \quad (24)$$

TABLE I. Values (Ref. 15) of the contact-density enhancement  $g(0; n_+, n_-)$  in a homogeneous two-component Coulomb-Fermi gas for different values of the electron density parameter  $r_s$  and the density ratio  $x = n_+/n_-$ .

$r_s$	$x \rightarrow 0$	$x = 0.5$	$x = 1$
1	2.16	1.91	1.81
2	3.97	3.37	3.07
3	7.35	5.67	5.0
4	13.11	9.22	7.87
5	24.3	13.75	11.5
6	40.4	20.8	16.4

where

$$a(n) = \frac{1}{n^3} [2k(n) - 6g_1(n) + 8g_2(n) - 2g_0(n)],$$

$$b(n) = \frac{1}{n^2} [-3k(n) + 11g_1(n) - 16g_2(n) + 5g_0(n)], \quad (25)$$

$$c(n) = \frac{1}{n} [k(n) - 4g_1(n) + 8g_2(n) - 4g_0(n)],$$

and  $g_0(n)$ ,  $g_1(n)$ , and  $g_2(n)$  are functions interpolating and extrapolating Lantto's data for  $n_+ \rightarrow 0$ ,  $n_+ = n_-$ , and  $n_+ = \frac{1}{2}n_-$ , respectively (see Appendix A and Fig. 7). The suitable extrapolation ensures the proper behavior of these functions for  $r_s \rightarrow 0$  [the random-phase-approximation (RPA) limit] and  $r_s \rightarrow \infty$  (the Ps limit). The function  $k(n)$  results from the continuity and symmetry of  $g(0, n_+, n_-)$  throughout the  $(n_+, n_-)$  plane and reads

$$k(n) = \frac{1}{2} n \frac{d}{dn} g_1(n). \quad (26)$$

For fixed  $n_+$  and  $n_-$  the two-component positron-electron contact amplitude is generally smaller than for one positron in a homogeneous electron gas of the same density, and varies smoothly with the ratio  $n_+/n_-$ . An example ( $r_s = 1$ ) of contact densities for various values of  $x = n_+/n_-$  is presented in Fig. 7.

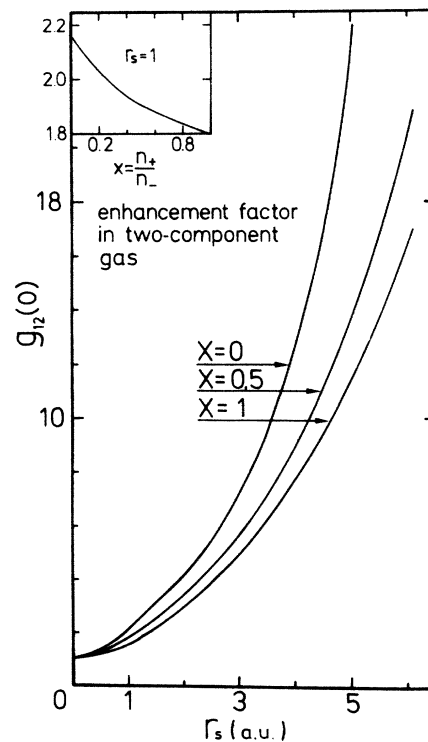


FIG. 7. The contact density  $g(0; n_+, n_-)$  in a homogeneous positron-electron gas for different values of  $r_s$  and the density ratio  $x = n_+/n_-$ .

### V. APPLICATION TO POSITRON TRAPPING AT VACANCIES

We have applied the full two-component scheme to the case of positron trapping at vacancies of simple metals such as Al, Zn, Cd, Mg, Hg, Li, and Na. The vacancies were modeled as spherical holes in the jellium background with

$$n_0(\mathbf{r}) = \frac{3}{4\pi r_s^3} \Theta(r - R_{WS}), \quad (27)$$

where  $R_{WS}$  is the Wigner-Seitz radius. Note that in this case ( $N_+ = 1$ ) the self-exchange-correlation potential  $\mu_{xc}(n_+(\mathbf{r}))$  in Eq. (3) is replaced by that for a fully-spin-polarized system ( $\mu_{xc}^F$ ), since the single positron has a well-defined spin. In order to obtain a realistic trapping potential for positrons, we mimic the repulsion<sup>3-6</sup> of the positron from the true host-ion cores by an added square-well potential for a positron. The values of the density parameter  $r_s$ , the valency  $Z$ , and the kinetic-energy well  $E_0$  are given in Table II, where also results for the calculated positron lifetimes and binding energies are presented. These latter values are compared with ones obtained when no crossterms are taken into account in the one-particle equations. A typical result is a greater binding energy for positron in vacancies in the full approach. Differences between these two cases are rather small for all metals, especially for those of greater  $r_s$ , although for some cases the change when applying the two-component approach is quite large. Only for aluminum is the new

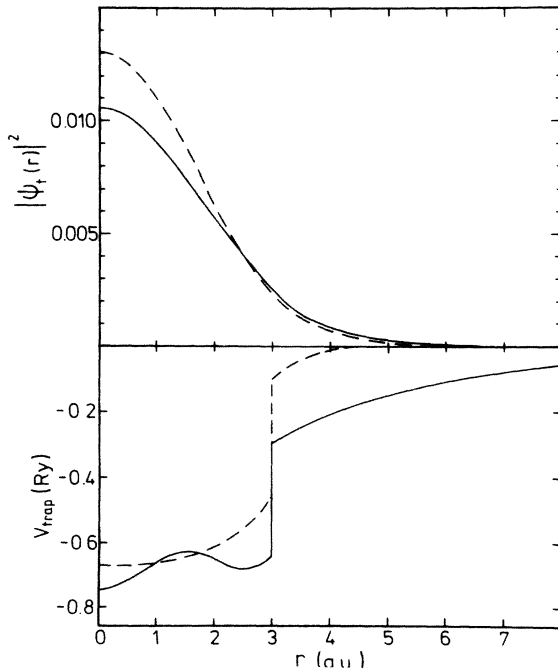


FIG. 8. The positron probability distribution  $|\psi^+(\mathbf{r})|^2$  and the effective trapping potential  $V_{\text{trap}}(\mathbf{r})$  for the Al vacancy. Solid curve, two-component density-functional theory; dotted curve, assuming no electron-density response to the entering positron.

TABLE II. Results of (a) the conventional and (b) two-component self-consistent calculations for positrons in metal vacancies approximated by the jellium model.  $r_s$  is the electron-density parameter,  $Z$  the valency, and  $E_0$  the depth of the kinetic-energy well (core repulsion).  $\tau$  denotes the positron-vacancy lifetime,  $E_b$  the positron binding energy, and  $E_T$  the total energy of the system, which in case (a) reduces to the sum of the vacancy-formation energy and positron-energy eigenvalue.

Metal	Al	Zn	Cd	Mg	Hg	Li	Na
$r_s$	2.07	2.31	2.59	2.65	2.65	3.25	3.93
$Z$	3	3	2	2	2	1	1
$E_0$ (eV)	4.8	4.6	4.4	3.1	4.2	1.7	1.7
	(a)	(a)	(a)	(a)	(a)	(a)	(a)
	(b)	(b)	(b)	(b)	(b)	(b)	(b)
$E_T$ (eV)	-3.77	-1.77	-1.37	-0.62	-1.22	0.18	0.31
	-5.36	-3.30	-2.60	-1.97	-2.41	-0.91	-0.63
$E_b$ (eV)	1.87	1.05	1.17	0.51	1.10	no positron	0.003
	1.59	1.53	1.23	1.35	1.19	1.09	0.94
$\tau$ (psec)	250	240	272	266	321	323	396
	240	272	266	315	317	358	421
						bound state	



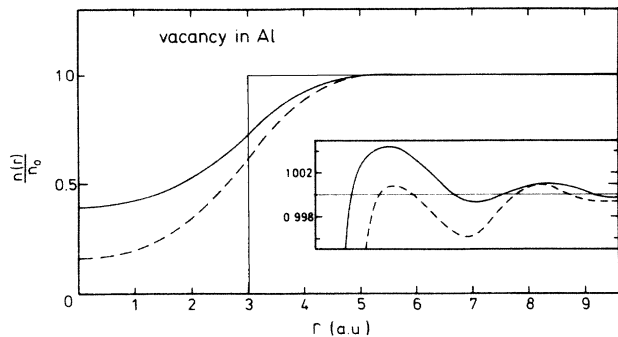


FIG. 9. The electron density at a vacancy in Al (jellium model). Solid curve, two-component density-functional theory; dotted curve, electron density in absence of the positron. The density is given in units of the bulk electron density  $n_0$ .

value of the binding energy somewhat smaller. There is a small difference between the present result for Al and the one presented earlier.<sup>32</sup> It is due to improvements in the electron-positron correlation energies and potential: the previous values were based on the VBS results. For Li no bound state is formed when the conventional approach is used. However, in the full two-component scheme, positron-electron correlation is greater and a bound state has appeared. For Na, when treating correlation conventionally, one obtains a very weak binding, which increases considerably in the two-component approach.

In the conventional calculation the effective trapping potentials for positrons are rather short ranged, whereas in the two-component case they are longer ranged. In Fig. 8 the effective potential for a positron in the Al vacancy is shown. It is nonmonotonous inside the vacancy, which is caused by the particular character of the potential  $\mu_+$  when both densities  $n_+$  and  $n_-$  are varying. It also ranges considerably further from the vacancy. The positron is a little less localized, as can be seen from Fig. 8, where  $|\psi^+(r)|^2$  is also plotted.

Figures 9 and 10 show the self-consistent electron density for a jellium vacancy in Al and Mg, both with and without a positron present. One can see the essential increase of  $n_-(r)$  inside the vacancy, and larger Friedel oscillations of the electronic charge outside. The change in  $n_-(r)$  from the conventional approach is presented in Fig. 11 for Al and Mg. Here one can also see the positron-

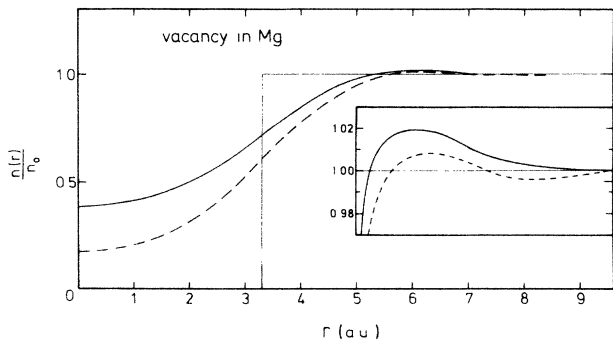


FIG. 10. As in Fig. 9, but for a vacancy in Mg.

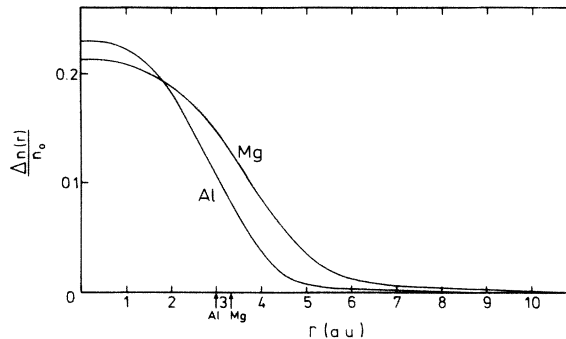


FIG. 11. Differences in electron density between conventional and two-component density-functional approaches; the curves for Al and Mg are taken as examples.

induced difference density  $\Delta n$  for both metals.

Figure 12 presents the contributions to the effective potential  $V_{\text{eff}}$  for electrons both for the two-component and the conventional approach. One can see that in the two-component scheme the scattering potential is weaker.

The positron trapping potential  $V_{\text{trap}}^{\text{eff}}$  is presented for Al in Fig. 13. One can see here again a change of the shape inside the vacancy. In the new approach  $V_c^{e-p}$  is essentially larger, but it is compensated to a high degree by the self-exchange and self-correlation contributions in-

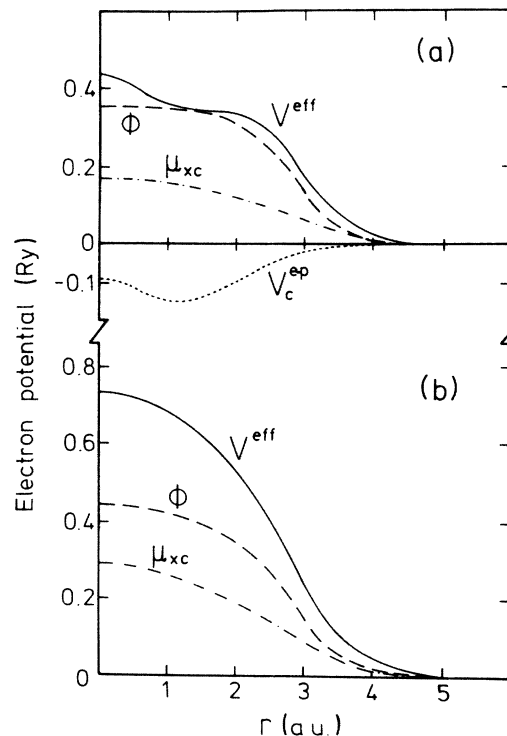


FIG. 12. Effective scattering potentials  $V_{\text{eff}}$  for electrons at the Al vacancy: (a) two-component density-functional approach; (b) conventional density-functional approach.  $\mu_{xc}$  is the exchange-correlation part and  $\phi$  the electrostatic part of the effective potential.  $V_c^{e-p}$  comes from electron-positron correlation in the two-component theory.

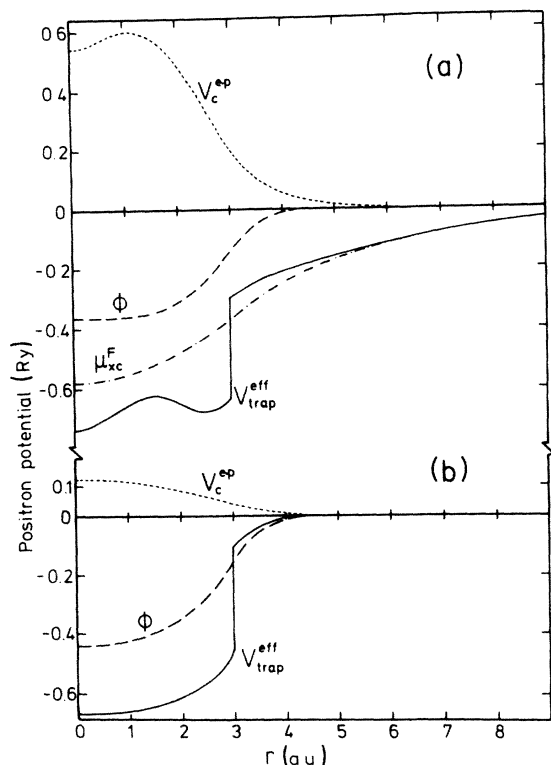


FIG. 13. Effective trapping potentials  $V_{trap}^{eff}$  for a positron in the Al vacancy: (a) two-component density-functional approach; (b) conventional density-functional approach.  $\phi$  is the electrostatic and  $V_c^{ep}$  the positron-electron correlation part of the effective potential.  $\mu_{xc}^F$  is the positron ferromagnetic, self-exchange correlation in the two-component scheme. The reduction in the positron kinetic energy which contributes to  $V_{trap}^{eff}$  is  $E_0=0.352$  Ry.

side the vacancy. Moreover, outside the vacancy the positron self-interaction has a long tail and, consequently, the effective trapping potential becomes long ranged. The self-interaction effects due to the LDA are discussed in Appendix B.

It is also very interesting to compare the lifetime values given by the two approaches (see Table II). Both compare well with experiment. The two-component calculations using Eq. (23) give values differing from the conventional ones by less than a few percent, even if the average density profiles are grossly different. This signals that, as far as the annihilation rates are concerned, there is a cancellation between (i) the electron pileup in the trap region due to the presence of the positron, and (ii) the diminished contact rate due to the nonzero positron density. This amounts to noting that in the vacancy the screening density is redistributed among the average component and the short-range enhancement.

## VI. SUMMARY

A general density-functional theory is presented for two-component Coulomb-Fermi systems. In particular, we have constructed the electron-positron (electron-hole) correlation-energy functional and its derivatives (the

correlation potentials) throughout the  $(n_+, n_-)$  plane. This construction is based on existing many-body calculations for the two limiting cases,  $n_+ \rightarrow 0$  and  $n_+ = n_-$ . Moreover, we discuss the complete phase diagram of the homogeneous electron-positron plasma. In addition, we present an interpolation formula for the contact density in the two-component mixture for use in annihilation-rate calculations.

The techniques are applied in fully-self-consistent calculations where the distorting effect of the localized (trapped) positron on the electron states in its vicinity is, for the time being, taken into account. The noteworthy feature is the interplay between the mean density *increase* and the *decrease* in the local-contact-density—enhancement factor (short-range screening). In the limit of very strong localization (e.g., by increasing the positive particle mass), the former term always dominates and one recovers the correct limit where the particle is treated as a static charged external perturbation. The calculations are performed for the model problem of positron trapping at simple metal monovacancies. The results show interesting cancellation effects; i.e., although the changes in both electron and positron densities from the conventional calculations (which partly ignore the cross correlations) are large, the changes in physical observables such as the annihilation rate or the binding energy are relatively small. This gives credence to the standard calculational techniques used in positron-defect spectroscopy. On the other hand, the present technique may soon find interesting new applications with the advent of the true electron-positron plasma experiments in the facilities for intense slow-positron beams. Such applications include various surface phenomena, many positrons confined into a single void, and various positron-ion complexes.

## ACKNOWLEDGMENTS

We are grateful to Lauri Lantto and Matti Manninen for many useful discussions. One of us (E.B.) acknowledges financial support from the Research Institute for Theoretical Physics at the University of Helsinki.

## APPENDIX A: INTERPOLATION FORMULAS

In this appendix we present some interpolation formulas for the electron-positron correlation energy in the case of one positron in a homogeneous electron gas, and in the case when the number of positrons equals the number of electrons. The formulas corresponding to the first case are based mainly on the results of Arponen and Pajanne<sup>1,22</sup> and those corresponding to the second make use of Lantto's<sup>15</sup> data and the results of Sec. II. The formulas have been derived so that the correlation-energy functional and its derivatives are continuous over the entire range of  $r_s$ .

### 1. Correlation energy of one positron in a homogeneous electron gas (in Ry)

We write, for  $r_s \leq 0.302$  (the RPA result),

$$\varepsilon^{e-p}(r_s) = -1.56/\sqrt{r_s} + (0.051 \ln r_s - 0.081) \ln r_s + 1.14.$$

For  $0.302 \leq r_s \leq 0.56$ ,

$$\varepsilon^{e-p}(r_s) = -0.92305 - \frac{0.05459}{r_s^2}.$$

For  $0.56 \leq r_s \leq 8.0$ ,

$$\varepsilon^{e-p}(r_s) = -\frac{13.15111}{(r_s + 2.5)^2} + \frac{2.8655}{r_s + 2.5} - 0.6298.$$

For  $8.0 \leq r_s < \infty$ ,

$$\varepsilon^{e-p}(n(r_s)) = -179856.2768n^2 + 186.4207n - 0.524.$$

## 2. Correlation energy for a fully compensated system ( $n_+ = n_-$ ) (in Ry)

We write, for  $0 \leq r_s \leq 0.8$ ,

$$\varepsilon^{e-p}(r_s) = -0.23831 + 0.07895 \ln r_s.$$

For  $0.8 \leq r_s \leq 6$ ,

$$\varepsilon^{e-p}(r_s) = -\frac{28.3225}{(r_s + 5.0)^2} + \frac{6.4466}{(r_s + 5.0)} - 0.52548.$$

For  $6 \leq r_s \leq 15.85$ ,

$$\varepsilon^{e-p}(r_s) = -0.307265 - 0.148162 \tanh[0.39145(r_s - 9.8)].$$

For  $r_s \geq 15.85$ ,

$$\varepsilon^{e-p}(r_s) = -0.50725 - 2\varepsilon_{CA}(r_s),$$

where  $\varepsilon_{CA}(r_s)$  is the result of Ceperley and Alder<sup>14</sup> as interpolated by Vosko *et al.*<sup>33</sup>

## 3. Contact density

The formulas for the contact density (the value of the pair-distribution function at the origin) are presented for the following cases: (A)  $n_+ \rightarrow 0$  (one positron in a homogeneous electron gas),

$$g_0(r_s) = 1 + 1.23r_s + 0.8295r_s^{3/2} - 1.26r_s^2 + 0.3286r_s^{5/2} + r_s^3/6,$$

(B)  $n_+ = n_-$ ,

$$g_1(r_s) = 1 + 0.51r_s + 0.65r_s^2 - 0.51r_s^{5/2} + 0.176r_s^3, \quad (\text{A3})$$

and (C)  $n_+ = \frac{1}{2}n_-$ ,

$$g_2(r_s) = 1 + 0.6r_s + 0.63r_s^2 - 0.48r_s^{5/2} + 0.167r_s^3.$$

The formulas are interpolations of Lantto's<sup>15</sup> results (Table I) preserving the proper behavior when  $r_s \rightarrow 0$  (RPA limit) and for  $r_s \rightarrow \infty$ .

## APPENDIX B: SELF-INTERACTION CORRECTIONS

For a positron trapped at a vacancy in Al, we have solved the self-consistent equations (2) and (3) also in the case where the positron self-interaction has been subtracted. Then, Eq. (3) for the positron is written as

$$\left[ -\frac{1}{2}\nabla^2 - \int d\mathbf{r}' \frac{n_-(\mathbf{r}') - n_0(\mathbf{r}')}{|\mathbf{r} - \mathbf{r}'|} + \frac{\delta E_c^{e-p}[n_+, n_-]}{\delta n_+(\mathbf{r})} \right] \psi^+(\mathbf{r}) = \varepsilon^+ \psi^+(\mathbf{r}), \quad (\text{B1})$$

and the change in the positron effective potential in relation to (3) is

$$\Delta V_{\text{eff}}(\mathbf{r}) = - \int \frac{n_+(\mathbf{r}')}{|\mathbf{r} - \mathbf{r}'|} d\mathbf{r}' - \mu_{xc}(n_+(\mathbf{r})). \quad (\text{B2})$$

After this correction, the positron effective potential becomes stronger (by  $\sim 20\%$  at the origin), and the positron-electron correlation part of this potential also grows up (by  $\sim 40\%$ ). The positron then becomes somewhat more localized at the vacancy, and attracts more electronic charge towards the center of the vacancy. However, the enhancement of the electron density inside a vacancy is very small and the net effect on positron lifetimes is nearly negligible (240  $\rightarrow$  243 psec). The change in the positron binding energy is from 1.59 to 1.12 eV. These comparisons are made with the calculations where crossterms and LDA self-interaction terms are included.

\*Permanent address: Institute for Low Temperature and Structure Research, Polish Academy of Sciences, 50-950 Wroclaw, Place Katedralny 1, Poland.

<sup>1</sup>J. Arponen and E. Pajanne, *Ann. Phys. (N.Y.)* **121**, 343 (1979).  
<sup>2</sup>S. Berko, in *Positron Solid State Physics*, edited by W. Brandt and A. Dupasquier (North-Holland, Amsterdam, 1983).  
<sup>3</sup>C. H. Hodges and M. J. Stott, *Phys. Rev. B* **7**, 73 (1973).  
<sup>4</sup>M. Manninen, R. Nieminen, P. Hautojärvi, and J. Arponen, *Phys. Rev. B* **12**, 4012 (1975).  
<sup>5</sup>R. P. Gupta and R. W. Siegel, *Phys. Rev. Lett.* **39**, 1212 (1977).  
<sup>6</sup>M. Puska and R. Nieminen, *J. Phys. F* **13**, 333 (1983).  
<sup>7</sup>C. H. Hodges and M. J. Stott, *Solid State Commun.* **12**, 1153 (1973); R. M. Nieminen and C. H. Hodges, *Phys. Rev. B* **18**, 2568 (1978).  
<sup>8</sup>*Theory of the Inhomogeneous Electron Gas*, edited by S. Lundqvist and N. H. March (Plenum, New York, 1983).

<sup>9</sup>R. M. Nieminen, in *Positron Solid State Physics*, Ref. 2.

<sup>10</sup>B. Chakraborty and R. W. Siegel, *Phys. Rev. B* **27**, 4535 (1983).

<sup>11</sup>See, e.g., A. P. Mills, Jr., in *Positron Scattering in Gases*, edited by J. W. Humberston and M. R. C. McDowell (Plenum, New York, 1984), p. 121.

<sup>12</sup>P. Vashishta, P. Bhattacharyya, and K. S. Singwi, *Phys. Rev. B* **10**, 5108 (1974).

<sup>13</sup>J. Rose and H. B. Shore, *Phys. Rev. B* **17**, 1884 (1978); M. Rasolt and D. J. W. Geldart, *ibid.* **15**, 979 (1977).

<sup>14</sup>D. M. Ceperley and B. L. Alder, *Phys. Rev. Lett.* **45**, 566 (1980).

<sup>15</sup>L. J. Lantto (unpublished); see also T. Chakraborty and P. Pietiläinen, *Phys. Rev. Lett.* **49**, 1034 (1982); P. Pietiläinen, L. Lantto, and A. Kallio, in *Recent Progress in Many-Body Theory*, Vol. 198 of *Lecture Notes in Physics*, edited by H.

- Kümmel and M. L. Ristig (Springer, Heidelberg, 1984), p. 181.
- <sup>16</sup>K. S. Singwi, M. P. Tosi, R. H. Land, and A. Sjölander, *Phys. Rev.* **176**, 589 (1968).
- <sup>17</sup>A. Sjölander and M. J. Stott, *Phys. Rev. B* **5**, 2109 (1972); P. Bhattacharyya and K. S. Singwi, *Phys. Lett.* **41A**, 457 (1972).
- <sup>18</sup>P. Bhattacharyya and K. S. Singwi, *Phys. Rev. Lett.* **29**, 22 (1972).
- <sup>19</sup>J. G. Zabolitzky, *Phys. Rev. B* **22**, 2353 (1980).
- <sup>20</sup>L. J. Lantto, *Phys. Rev. B* **22**, 1380 (1980).
- <sup>21</sup>A. Kallio, P. Pietiläinen, and L. J. Lantto, *Phys. Scr.* **25**, 943 (1982).
- <sup>22</sup>J. Arponen and E. Pajanne, in *Proceedings of the 7th International Conference on Positron Annihilation, New Delhi, India, 1985* (World-Scientific, Singapore, in press).
- <sup>23</sup>W. F. Brinkman and T. M. Rice, *Phys. Rev. B* **7**, 1508 (1973).
- <sup>24</sup>T. M. Rice, in *Solid State Physics*, edited by H. Ehrenreich and D. Turnbull (Academic, New York, 1977), Vol. 32.
- <sup>25</sup>W. F. Brinkman, T. M. Rice, and B. Bell, *Phys. Rev. B* **8**, 1570 (1973).
- <sup>26</sup>A. Akimoto and E. Hanamura, *J. Phys. Soc. Jpn.* **33**, 1537 (1972).
- <sup>27</sup>J. Shy-Yih Wang and C. Kittel, *Phys. Lett.* **42A**, 189 (1972).
- <sup>28</sup>D. N. Lowy and A. D. Jackson, *Phys. Rev. B* **12**, 1689 (1975).
- <sup>29</sup>W. Kohn and C. Majumdar, *Phys. Rev.* **138A**, 1617 (1965).
- <sup>30</sup>E. Boronski and R. M. Nieminen, in *Proceedings of the 7th International Conference on Positron Annihilation, New Delhi, India, 1985*, Ref. 22.
- <sup>31</sup>W. Brandt and J. Reinheimer, *Phys. Lett.* **35A**, 109 (1971).
- <sup>32</sup>R. M. Nieminen, E. Boronski, and L. Lantto, *Phys. Rev. B* **32**, 1377 (1985).
- <sup>33</sup>S. H. Vosko, L. Wilk, and M. Nusair, *Can. J. Phys.* **58**, 1200 (1980).